ELSEVIER

Computerized Medical Imaging and Graphics 28 (2004) 51–59

Computerized Medical Imaging and Graphics

www.elsevier.com/locate/compmedimag

Tracking deforming aortas in two-photon autofluorescence images and its application on quantitative evaluation of aorta-related drugs

Jue Wang[a], Liang Ji[a,*], Xing-Sun Lin[b], Hui Ma[b]

[a]*Department of Automation, Tsinghua University, Beijing 100084, China*
[b]*Department of Physics, Tsinghua University, Beijing 100084, China*

Received 1 October 2002; accepted 4 April 2003

Abstract

This paper describes a novel approach to an objective measurement of aorta samples of rats and a quantitative evaluation of aorta-related drugs. Two-photon fluorescence microscopy is used for recording image sequences of deforming aorta. Time sequence snake models are used to track the structural deformations of aorta walls caused by drug stimulation of the elastic lamina in the aorta. Several objective and quantitative biomarkers extracted from these models are used as diagnostic indicators. In a preliminary study, the technique was successfully used for evaluating the effect of a newly developed drug—human erythrocyte-derived depressing factor quantitatively and objectively.

Keywords: Two-photon autofluorescence imaging; Aorta; Quantitative evaluation; Time sequence snake model; Human erythrocyte-derived depressing factor

1. Introduction

Modern biomedical research has benefited from a renaissance in light microscopy, brought about by the convergence of developments in the fields as diverse as electronics, optics, molecular biology, computer science, and reagent chemistry. Integration of these has transformed microscopy into a highly useful and dynamic research tool for biology and medicine. It is now possible to generate highly resolved functional maps of molecular events in living organisms where new types of specimens can be studied quantitatively and non-invasively with greatly improved spatial and temporal resolution.

Invented by Webb in 1990, two-photon fluorescence microscopy (TPM) has been considered a revolutionary development in bioimaging [1,2]. The technique is based on the non-linear excitation of fluophores and is capable of producing deeper penetration and better resolution in optically turbid biological specimens, such as tissues. The use of infrared light for excitation leads to reduced photon damage to living samples. In a previous attempt, TPM was successfully applied to obtain autofluorescence images of elastic lamina in rat aorta [3]. Features extracted from these images suggest correlations between the morphology of the elastic lamina and the pathological status of the aorta [4].

Although these images may contain rich features for diagnostic applications, retrieving the information is not trivial. Information obtained from visual examination by pathologists is often subjective, qualitative and heavily depends on personal experiences. There is an urgent demand for extracting objective and quantitative biomarkers from such images and using them as diagnostic indicators. Although multi-photon imaging has been successfully applied to some specific biological studies [5–7], unfortunately, there has been no emphasis on objective biomarker extraction and quantitative analysis.

The motivation behind this work is to develop new methods for monitoring and quantitative analysis of aorta-related drug effects on living tissues. The arterial wall of specimen contains elastic lamina, which plays the most important role in determining the physiological function of the aorta. It has been observed in our previous experiments that under the drug stimulation, living aorta samples will produce a sudden structure deformation caused by the shrinkage of internal elastic lamina, followed by a relatively gently reversion process. The whole deformation typically lasts for 4–5 min and can be recorded by TPM, benefited from its minimum damage to living samples. It has also

* Corresponding author. Tel.: +86-10-62785787; fax: +86-10-62794295.
E-mail addresses: zc-sa@tsinghua.edu.cn (L. Ji); mahui@tsinghua.edu.cn (H. Ma).

0895-6111/$ - see front matter © 2003 Elsevier Ltd. All rights reserved.
doi:10.1016/j.compmedimag.2003.04.001

been observed that when adding different drugs to aorta samples, the deformation processes are usually different. This important fact provides us an opportunity to compare different drugs by analyzing the corresponding aorta deformations. For the purpose of objectivity and quantitativeness, a time sequence active contour model is proposed to track the vascular wall and their activities in image sequences. Active contour, also called 'snake', was first introduced by Kass [8]. Due to its intrinsic ability to handle variations of the boundary, it has been widely used to solve problems such as boundary detection and object extraction [9,10], especially in medical and biological imaging applications [11,12]. In our approach, the time sequence snake model is a combination of 1D boundary representation of 2D shape [13] and the regular snake. It is not only able to locate the aorta in each image, but also provides a rich collection of biomarkers that can be used to describe the deformations of arterial walls in time image sequence. Experiments on a newly developed drug human erythrocyte-derived depressing factor (EDDF) show that these biomarkers work well as diagnostic indicators and can be used effectively for the evaluation of aorta-related drug effects.

The layout of the paper is as follows. In Section 2, an overview of two-photon fluorescence imaging and materials used in our experiments are given. Section 3 discusses the proposed time sequence snake model and several valuable biomarkers extracted from it. In Section 4, the experimental results are presented. A discussion on these results is given in Section 5.

2. Two-photon fluorescence imaging and materials preparation

2.1. Two-photon fluorescence imaging

The experimental set up is the same as described previously [3]. Autofluorescence image sequences of aorta samples were recorded using a BioRad MRC-1024MP two-photon microscope. A mode-locked Ti:Sapphire laser (Spectral Physics Millennium X pumped Tsunami Lite) provided the excitation beam, as shown in Fig. 1. For two-photon excitation, the laser was operated at 800 nm with about 100 fs pulse width. A $\times 10$ 0.25 N.A objective lens was used in all measurements. Pulse width at the sample was estimated to be around 200 fs. Fluorescence was collected through a 460 nm long-pass filter (Chroma).

2.2. Human erythrocyte-derived depressing factor

The drug evaluated in our experiments was extracted from human red blood cells for the first time by Dr Wen and was named erythrocyte-derived depressing factor or EDDF [14]. EDDF exists in human beings and other kinds of animals, including pig, dog, rat, rabbit, cow and so on. It is present in both erythrocytes and tissues such as brain, heart, liver and kidney. Previous studies showed that it could significantly decrease blood pressure in several experimental hypertensive models and was very safe with LD50 (50% lethal dose) greater than 1500 mg/kg. Further studies suggested that the action mechanisms of EDDF were closely related to vasodilation in an endothelium dependent manner, which might be mediated by endothelium-derived relaxing factor-NO-cGMP pathways and significantly decreasing cytosolic and nuclear Ca^{2+} levels in vascular smooth muscle cell. Although the toxicity, the physical and chemical characteristics and the mechanisms of this drug has been tested in previous studies, effects of it on living tissues has not been observed directly and analyzed quantitatively.

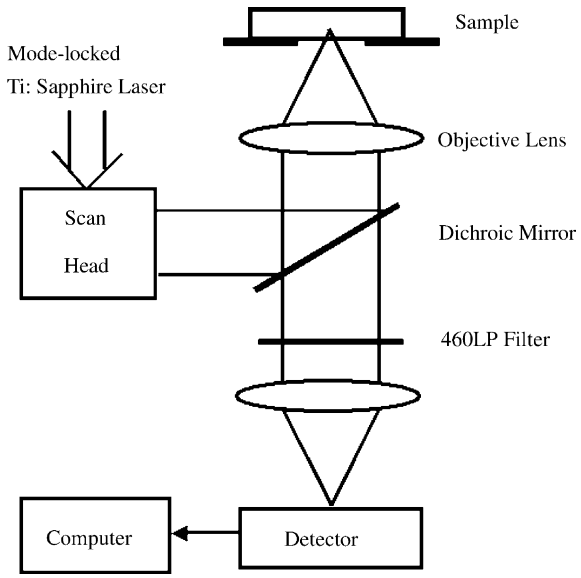

Fig. 1. Sketch map of the two-photon autofluorescence microscopy.

2.3. Experimental methods

The experiments were carried out on the abdominal aortas of calcium overload Wistar male rats (180–220 g). After a rat was sacrificed, its mesentery and abdomen aortas were removed quickly and rinsed in PSS solution to remove blood residue. The aortas were then cut laterally to rings of 1–2 mm width and kept in Petri dishes filled with PSS solution. Before being imaged, these samples had to be incubated in 37 °C, 5% CO_2 environment for 1–2 h to release the internal tension while keeping their biological functionality. The aorta rings were then placed separately at the bottom of the Petri dish with the cut cross section down for two-photon autofluorescence imaging. Each ring was submerged by a small droplet of PSS solution. The Petri dish was then filled with paraffin wax to prevent the PSS droplet from drying out and to keep the droplet stable during imaging. Note that in our study, the aortic tissues were kept

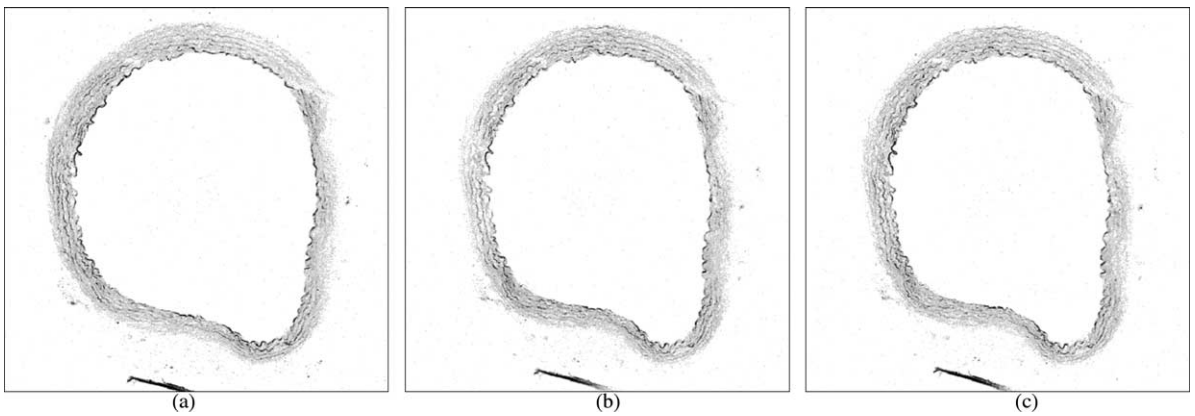

Fig. 2. Sample frames extracted from an image sequence. Different structures of the aorta in these images indicate the deformation of it due to drug stimulation. (a) $t = 0$, the first frame. (b) $t = 250$ s, the 41st frame. (c) $t = 500$ s, the 66th frame.

alive with their physiological function maintained, although rats were dead before experiments.

In the experiments, intensive contractions in mesenteric artery rings were observed after they were stimulated by some vasoactive agents such as HiK^+ and norepinephrine (NE). Since EDDF can significantly relax vascular smooth muscle and plays a role as a protector, it is natural to suppose that after the treatment with EDDF, artery rings will produce relatively subtle contractions under the HiK^+ or NE stimulation. To prove this, aorta samples were divided into two groups: the treatment group and the control group. Samples of the treatment group were incubated with EDDF (1 mg/ml) for about half an hour before experiments, while those of the control group were not. In each experiment, the aorta sample was firstly imaged for 100 s to check possible spontaneous contraction or relaxation. Once the ring became stable, HiK^+ or NE was then injected slowly through a micro-injector into the PSS droplet which wrapped the sample. Any deformation of the ring was recorded continuously during and after the injection. Fig. 2 shows some examples of such recorded image frames with $t = 0$ as the moment of drug injection. These results show that the structural deformations of aorta rings were noticeable but their changes with time were not obvious. All image sequences were processed and analyzed using the time sequence snake model, which will be discussed in detail in Section 3. Due to the intrinsic mechanisms of EDDF, aortic deformations of the experiment and the control group were expected to be different. By analyzing biomarkers extracted from these deformations, the effectiveness of the drug can be distinguished clearly, and more important, quantitatively and objectively.

3. Time sequence snake models

3.1. Single frame snake models

Autofluorescence aorta images collected in our experiments usually have high signal-to-noise ratios due to the powerful capability of the TPM, as shown in Fig. 2. There is also enough prior knowledge about aorta rings. For example, they usually have elliptical or circular shapes. Given the quality of the images and the prior knowledge, it seems quite easy to segment aorta rings from these images. Indeed in our preliminary attempts, some straightforward methods were tested. They are described as follows.

Thresholding was applied firstly to extract the main body of the aorta ring from the image. The threshold was selected automatically to make the aorta body have a fixed area ratio to the whole image. To eliminate noise around the boundary of the aorta, morphological operations such as opening and closing [15] were applied, followed by a labeling operation. After these simple and fast operations, the aorta ring was roughly located and an estimation of the body of the ring was obtained. A centroid-to-boundary method was then used to draw the inner boundary of the aorta, as shown in Fig. 3. The centroid of the image was also viewed as the centroid of the ring. A series of radials were drawn from the centroid and ended at the inner boundary of the aorta. These intersection points were then connected as an estimation of the inner boundary of the ring.

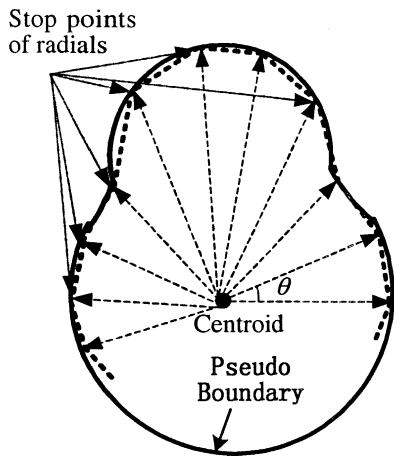

Fig. 3. The straightforward centroid-to-boundary method for inner aorta boundary extraction. This method will be failed frequently in our situation.

Although this method works well in some situations, it frequently fails in others. The major problem of the method is that in some images, parts of the aorta ring are blurred caused by ring contraction and the corresponding boundary cannot be observed. For this reason, using local detection methods only is insufficient to extract whole aorta boundary and some global optimization methods must be employed.

To give reasonable segmentation results, snake models are used for aorta tracking, which have already been successfully used for the similar purpose in MR images [16] and CT images [17]. Snake is the energy-minimizing spline guided by internal constraint forces and influenced by external image forces that pull it toward lines and edges. A snake is an ordered set of points denoted as $V = [v_1, v_2, \ldots, v_n]$, where each snaxel v_i is defined on the 2D finite grid: $v_i \in E \equiv \{(x, y) : x, y = 1, 2, \ldots, M\}$. The internal and external energy of the snake is denoted as E_{int} and E_{ext}. The snake transfers the boundary extraction problem into an energy minimization problem and the boundary can be obtained by

$$V_\Lambda = \arg\min_V \sum_{i=1}^{N_s} \lambda_i E_{\text{int}}(v_i) + (1 - \lambda_i) E_{\text{ext}}(v_i) \tag{1}$$

where $\lambda_i \in [0, 1]$ are the regularization parameters, N_s is the number of snaxels in the snake. In our approach, we use the regular snake formula described in Ref. [8] for single image frame since it already yields promising segmentation results. However, using the snake in each image separately is still insufficient for extracting the characteristics of the aorta deformation process.

3.2. Time sequence snake models

In this study, a rich set of characteristic features are ensconced in the real-time sequence of aorta images, which typically includes more than 80 frames. To analyze such a sequence of images rather than a single frame, a time sequence snake model is developed based on the regular snake model described in Section 3.1 and important prior knowledge of aorta images were collected. Comparing with the speed of image capture, the deformations process of aortas is slow, so that the difference between aorta structures extracted from adjacent frames in the time sequence is usually small. The centroid-to-boundary concept is used for modeling the deformation of the aorta, as shown in Fig. 4. The ith snaxel in the snake has a fixed central angle $\theta_i = 2\pi i/N_s$, which enables the 2D shape to be represented by a 1D centroid-to-boundary distance function. For a snaxel v_i, its movement from time t to time $t + 1$ can be measured by

$$v_i(t+1) = \Delta d_i \frac{v_i(t) - O}{\|v_i(t) - O\|}, \qquad i = 1, \ldots, N_s \tag{2}$$

where Δd_i is the displacement of the snaxel along the radius between the snaxel in question and the centroid O during the time interval $[t, t + 1]$. In this way, the regular snake model

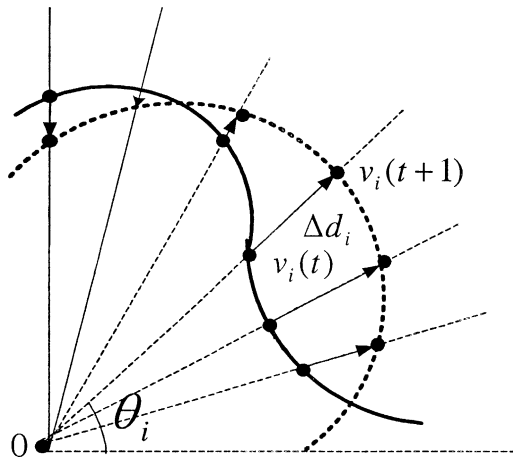

Fig. 4. Illustration of the time sequence snake model. Each snaxel on the snake has a fixed central angle in all frames in an image sequence.

evolves to a time sequence snake model and yields not only satisfying segmentation results but also a rich set of biomarkers in our specific case. Obviously, the accuracy of the model heavily depends on the number of snaxels in the snake. If snaxels are distributed too sparsely, the snake cannot represent the boundary very well and if they are distributed too densely, the snake will be largely affected by local image noise. To select the number of snaxels properly, a mismatch criterion minimization algorithm is proposed. We first select several representative images from the image sequences and manually mark enough points to represent the inner shape of the aorta ring in each image. These shapes are denoted as $S^i_{\text{manual}} = \lfloor s^i_1, s^i_2, \ldots, s^i_w \rfloor$, $i = 1, 2, \ldots, N_I$, where N_I is the number of images we selected, w is the number of points in each boundary. The jth points in each shape has a fixed central angle $\theta_i = 2\pi j/w$. The algorithm is formally described as follows:

(A) Set $N_s = n$ initially to make $n \ll w$.
(B) Calculate the snake in each image. After the snake is stable, sample w points along the snake, denoted as $S^i_{\text{snake}} = \lfloor \sigma^i_1, \sigma^i_2, \ldots, \sigma^i_w \rfloor$, $i = 1, 2, \ldots, N_I$. The jth points in each vector has a fixed central angle $\theta_i = 2\pi j/w$.
(C) Calculate the following mismatch criterion:

$$E_s = \frac{1}{N_I} \sum_{i=1}^{N_I} \left[\frac{1}{w} \sum_{j=1}^{w} \|\sigma^i_j - s^i_j\| \right] \tag{3}$$

(D) If E_s is diminished, set $N_s = N_s + 1$ and return to (B), otherwise quit the algorithm.

Another advantage of the proposed time sequence snake is that the initialization and the energy minimization process of it are simplified. Since the aorta structures of adjacent frames differ only slightly, snake of the current frame can be directly used as the initial position of the next frame. Furthermore, in a regular snake model, energy minimization needs exhaustive search in each snaxel's neighborhood and

therefore, it is very time-consuming. In the proposed model, each snaxel can only move towards one of two possible directions and the computation complexity is reduced dramatically. It makes the time sequence snake model more efficient and suitable for real-time processing.

In the proposed model, the centroid of the aorta is considered as stable and the motion of the aorta as a whole is discarded. However, the aorta ring will be impacted by the drug drop in the experiment and will generate a slight movement toward a certain direction. Such motion contains no useful information about the deformation but it would affect the calculation of biomarkers if it had not been removed before biomarker extraction. An image registration algorithm based on the time sequence snake is proposed to solve this problem. The position of the centroid of the aorta at the time t is defined as $g(t)$ and the global movement of the aorta during the time interval $[t, t+1]$ is defined as

$$\Delta g(t, t+1) = g(t+1) - g(t) \tag{4}$$

The deformation variance during the time interval is defined as

$$\Delta V(t, t+1) = \sum_{i=1}^{N_s} \|v_i(t+1) - v_i(t) - \Delta g(t, t+1)\|^2 \tag{5}$$

The global movement can be obtained by seeking a solution for

$$\{\Delta g(t, t+1)\} = \arg \min_{\Delta g(t,t+1)} \Delta V(t, t+1) \tag{6}$$

Because of the small difference between adjacent frames, only a few neighbors of $g(t)$ needs to be searched to determine the location of $g(t+1)$.

3.3. Biomarker extraction

The time sequence snake model provides rich features of the deformation of the aorta ring. Based on their properties, these biomarkers can be classified into three categories: geometrical features, energy features and motorial features.

Typical geometrical features include perimeter, area, contour ratio and so on. The calculation of these parameters is carried out on the inner boundary of the aorta located by the snake. The perimeter is calculated as

$$P = \sum_{i=1}^{N_s} \|v_i - v_{i-1}\|, \qquad v_0 = v_{N_s} \tag{7}$$

The area is calculated as

$$A = M + K - 1 \tag{8}$$

where M is the total number of pixels enclosed by the snake, and K is the total number of pixels on the snake curve. The contour ratio is defined as

$$C = \frac{P^2}{4\pi A} \tag{9}$$

It indicates the smoothness of the boundary and how it is close to a circle.

Extracting energy features of the snake is a natural consideration since the snake model is built on the concept of energy minimization. The internal energy of a single snake $V(s)$ in Ref. [8] is composed of its first and second derivatives denoted as

$$E_{\text{int}} = (\alpha |V_s(s)|^2 + \beta |V_{ss}(s)|^2)/2 \tag{10}$$

where α and β are weight factors. However, this kind of energy definition is meaningless in our situation since it is only related to the snake shape in a single frame. In our case, the energy must be defined on the whole image sequence to capture the characteristics of the aorta deformation. Since the intension in the aorta ring is released before experiment, we define the initial location of the aorta ring as a zero potential energy position. To describe the cumulated potential energy during the deformation process, a global internal energy for each snaxel is introduced as

$$E_g(v_k^i) = \frac{\|v_k^i - v_1^i\|^2}{l(V_k)} \tag{11}$$

where v_k^i denote the ith snaxel of the kth snake curve in the sequence, $l(V)$ is the average snaxel distance:

$$l(V_k) = \frac{1}{N_s} \sum_{i=1}^{N_s} \|v_k^i - v_k^{i-1}\|^2, \qquad v_k^0 = v_k^{N_s}. \tag{12}$$

The average global internal energy of the kth frame is calculated as

$$E_g(V_k) = \frac{1}{N_s} \sum_{i=1}^{N_s} E_g(v_k^i). \tag{13}$$

Motorial features provide motorial information of snaxels during deformation. Since the deformation of the aorta is typically slow, the sampling frequency can be easily controlled to avoid under-sampling problem. For a snaxel v_i, its velocity and acceleration at time t are denoted as u_i^t and a_i^t, and satisfy the motion equations:

$$\Delta d_i^t = u_i^t \Delta t + \frac{1}{2} a_i^t \Delta t^2 \tag{14}$$

$$u_i^{t+1} = u_i^t + a_i^t \Delta t \tag{15}$$

where Δd_i^t is the displacement of the snaxel in the time interval Δt.

Current location of the snake will influence its future position. The dynamic equation of the motion of the snake in the ith frame is:

$$\frac{\partial^2 V_i}{\partial t^2} = -\lambda \frac{\partial V_i}{\partial t} + F_i(V_i) \tag{16}$$

where λ is a coefficient related to the physical property of the aorta. By solving the equation, the force $F_i(V_i)$ is calculated from each frame and is used as a direct measure of the internal physical force during the deformation.

4. Results

Biomarkers were extracted using the models and methods described above and were plotted as a function of time. Some parameters were normalized to eliminate effects due to the large diversities among different samples. For a biomarker P, its value in each frame in an image sequence is denoted as $P(i)$, $i = 1, \ldots, n$ and is normalized as

$$P'(i) = P(i)/P_{\max}, \qquad P_{\max} = \text{Max } P(i) \tag{17}$$

Most of the biomarkers have strong correlations with the structural deformations of aorta rings caused by the drug stimulation. Because of the limitation of space, only a part of them are drawn in Fig. 5. It suggests that the proposed techniques are capable of detecting small deformations of aorta rings, even in the situation where the deformation is indistinguishable by human eyes.

Biomarkers extracted from both the treatment group and the control group are compared in Fig. 6. To make the biomarker values calculated from different image sequences comparable, another normalization method is employed. For a biomarker P, its values calculated from the experiment and the control group are denoted as $P_E(i)$ and $P_C(i)$. Then the maximum and minimum values of P in each group are obtained as

$$P_{E/C}^{\text{Max}} = \text{Max}(P_{E/C}(i)), \quad P_{E/C}^{\text{Min}} = \text{Min}(P_{E/C}(i)), \quad i = 1, \ldots, n \tag{18}$$

The biomarker values are normalized as

$$P'_{E/C}(i) = \begin{cases} P_{E/C}(i)/P_{E/C}^{\text{Max}}, & \text{if } P_{E/C}^{\text{Min}} > 0 \\ P_{E/C}(i)/\text{Max}(P_E^{\text{Max}}, P_C^{\text{Max}}), & \text{if } P_{E/C}^{\text{Min}} = 0 \end{cases} \tag{19}$$

It suggests that the contraction of the aortas in the treatment group is significantly reduced compared with those in the control group. Since the only difference between aortas in different groups is that the samples in the treatment group have been incubated with EDDF

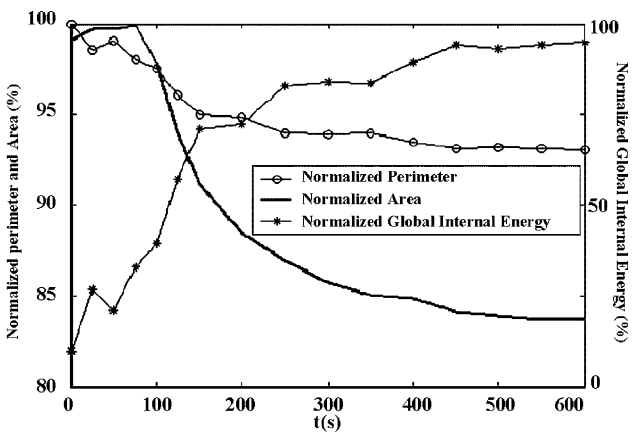

Fig. 5. Biomarkers extracted from the image sequence are normalized and plotted against time. Changes of these biomarkers give a quantitative description of the deformation of the aorta.

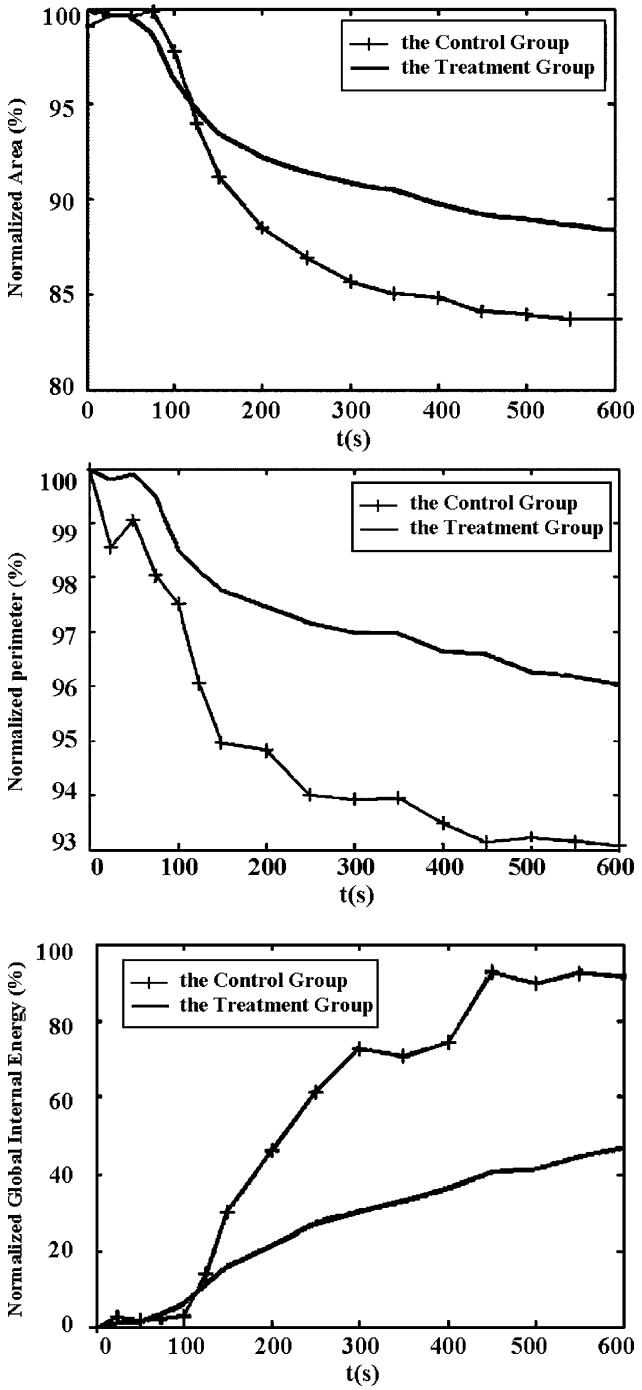

Fig. 6. Normalized biomarkers vs. time. (a). Normalized area. (b). Normalized perimeter. (c). Normalized global internal energy. The significant dynamic differences between biomarkers extracted from the treatment group and the control group give a quantitative evaluation of the drug EDDF.

while samples in the control group have not, it can be concluded that EDDF can effectively improve blood vessel reactivity of calcium overload rats to vasoactive agents.

To be more convincing, many groups of experimental results have been combined to extract some statistically

Table 1
DRREC values of seven biomarkers averaged from 18 groups of experiments. These values give a quantitative evaluation of the drug EDDF

	Perimeter	Area	Contour ratio	Global internal energy	Absolute velocity	Absolute acceleration	Absolute force
DRREC	0.59 ± 0.06	0.70 ± 0.04	0.81 ± 0.05	0.56 ± 0.04	0.84 ± 0.05	0.78 ± 0.04	0.82 ± 0.05

valuable numeric indicators. For a biomarker P, its normalized values calculated from the experiment and control group using Eq. (19) are denoted as $P'_{\mathrm{E}}(i)$ and $P'_{\mathrm{C}}(i)$. A new parameter named Dynamic Range Ratio of the Experiment Group to Control Group (DRREC) is defined as

$$\mathrm{DRREC} = \frac{\left(\mathrm{Max}(P'_{\mathrm{E}}(i)) - \mathrm{Min}(P'_{\mathrm{E}}(i))\right)}{\left(\mathrm{Max}(P'_{\mathrm{C}}(i)) - \mathrm{Min}(P'_{\mathrm{C}}(i))\right)} \tag{20}$$

Obviously, DRREC < 1 indicates that the drug has worked in the experiments and a smaller value of DRREC indicates a higher effectiveness of the drug. Table 1 shows the DRREC values of seven biomarkers we extracted. Each value was calculated by averaging the experimental results of three groups of rats, including 18 pairs of aortas. These statistical results show the effectiveness of EDDF clearly, numerically and objectively.

5. Discussion

The success of the proposed approach has benefited mainly from two important factors: the two-photon fluorescence imaging technique and the snake model based quantitative analysis method. The former provides us a powerful tool for on-line observation of living tissues and their physiological activities, while the latter enables us to track aortas in image sequences and to model their deformations. Biomarkers extracted from the model work well in our experiments on giving quantitative evaluations of aorta-related drugs.

However, a common problem of this type of work is the uncertainty to some extent of whether the differences presented in the experiments are due to artifacts of the algorithms or are produced by biological factors. Generally speaking, there are three major types of possible artifacts of the algorithm that may cause some uncertainties in the results, and listed as below.

1. The snake model may fail completely in dealing with some images, resulting in a large fluctuation of some biomarkers.
2. Although the snake can segment aorta walls quite well, there is always some mismatch between the extracted aorta boundary and its real location. This kind of mismatch may affect the results.
3. Some biomarkers such as the internal energy of the snake can be defined differently. If their definitions are changed, the difference between the control and the treatment group may disappear.

The first type of artifact can be excluded statistically by a large amount of experiments. Since the DRREC value of each biomarker we presented is calculated from 18 separate experiments, it cannot be claimed as an outcome of pure accidents. Besides, extracted biomarkers are also checked for large fluctuation between adjacent frames and if the abnormal fluctuation occurs, the total image sequence will be abandoned to avoid errors.

The possibility of the second type of artifact can also be excluded by statistical methods. The mismatch between the snake and the actual boundary of aorta ring can be viewed as algorithm noise. Although it will affect the calculation of biomarkers in a single image, it will be statistically diminished in the final DRREC values. To check whether this kind of noise is typically small, a comparative experiment was done. Three aorta rings were used in the experiment, denoted as aorta A, B and C, respectively. Aorta A was treated in the same way as those in the treatment group, stimulated by HiK^+ after incubated with EDDF. Aorta B was only stimulated by HiK^+ without EDDF, as those in the control group. Aorta C was only incubated with EDDF and was not stimulated during the experiment. It was used to test to what extent the biomarkers will fluctuate due to only algorithm artifacts. Values of the biomarker area calculated from the three aortas were plotted against time and compared in Fig. 7. It suggests that the biomarker fluctuation purely produced by algorithm artifacts is very small and the changes of biomarkers are mainly

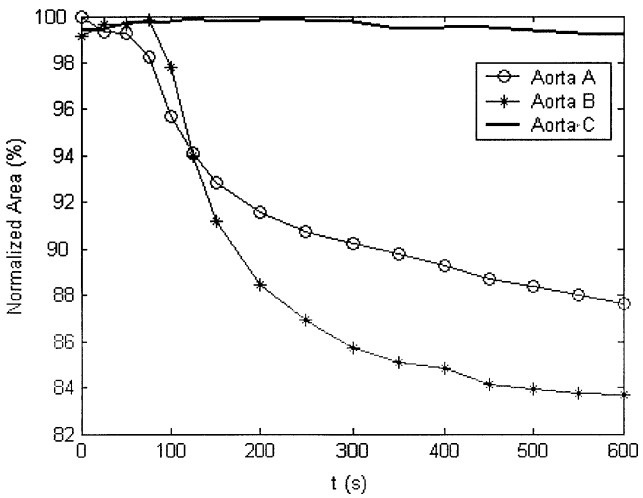

Fig. 7. Normalized area vs. time of three aortas: aorta A (stimulated by HiK^+ after incubated with EDDF), aorta B (stimulated by HiK^+ only) and aorta C (incubated with EDDF only). Since aorta C is not stimulated, the fluctuation of the biomarker extracted from it reflects only computational noise. It suggests that the difference between biomarkers extracted from A and B is so significant that cannot be claimed as algorithm artifacts.

produced by the HiK^+ or NE stimulation. Furthermore, the difference between the treatment group and the control group is so significant that it cannot be produced by the mismatch of the algorithm.

It is true that there are so many ways to define the internal energy of a snake and we cannot give each a test. In fact, there is no need for such an exhaustive test. Since the effectiveness of EDDF has already been approved by chemical and biological experiments, the fundamental goal of our work is to extract valuable and meaningful biomarkers, which can give a quantitative and objective evaluation of its effects on living tissues. Although numerous features can be extracted from these images, only those that are sensitive to the deformation of the aortas and are physically meaningful can be used as biomarkers and others will be discarded. To demonstrate that there are also other features that can be used as biomarkers, we modified our energy definition for another test. The global internal energy defined in Eqs. (11) and (13) is a potential energy; we changed it slightly to give a global kinetic energy which mainly focuses on kinetic information of the deformation. The energy is defined as

$$E'_{\mathrm{g}}(v_k^i) = \frac{\|v_k^i - v_{k-1}^i\|^2}{l(V_k)} \tag{21}$$

The global kinetic energy is calculated as

$$E'_{\mathrm{g}}(V_k) = \frac{1}{n}\sum_{i=1}^{n} E'_{\mathrm{g}}(v_k^i) \tag{22}$$

where parameters i, k and $l(V)$ are the same as those in Eqs. (11) and (13). The global kinetic energy of the treatment group and the control group is plotted against time in Fig. 8. Although the definition of the energy is changed, the significant difference between the treatment and the control group still exists. This experiment makes it more convincing that this kind of difference is introduced mainly by EDDF rather than algorithm itself.

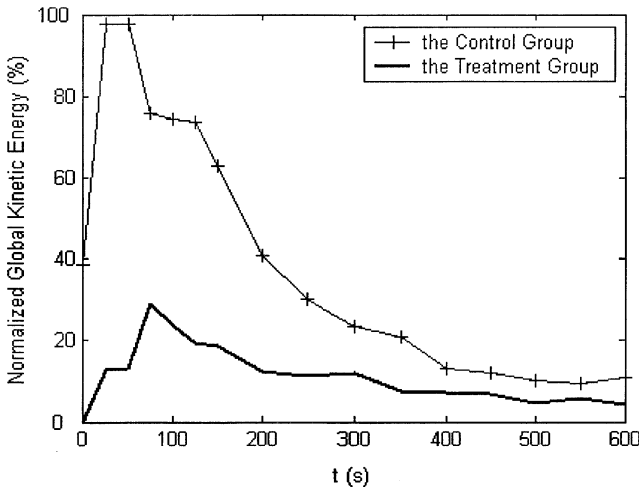

Fig. 8. The modified global internal energy is plotted against time. It is shown that the significant difference between the treatment and the control group still exists.

It should also be pointed out that currently all biomarkers we used are extracted from the time sequence snake model. They provide good description of deformation characteristics of aorta rings under drug stimulation in our experiments, but the relationships between some of the biomarkers and the biomechanical properties of the aorta are still unknown. More works are underway to setup quantitative relationship between the extracted biomarkers and some biomechanical parameters of the aorta obtained by other biomechanical experiments.

6. Summary

In this paper, an objective and quantitative evaluation method is proposed for aorta-related drugs, by combining advanced modern optical techniques and quantitative analysis methods. Two-photon excitation fluorescence microscopy is used for recording time sequence autofluorescence images of rat aorta. It has the advantage of less invasiveness and enables biological samples to maintain their physiological functions during experiments. Features in these images suggest correlations between the morphology of the elastic lamina and the pathological status of the aorta.

For the purpose of objectivity and quantitativeness, a time sequence active contour model is proposed to track the vascular wall and their activities in image sequences. By combining 1D boundary representation of 2D shape, single frame snake model evolves to a time sequence snake model and it not only is able to locate the aorta wall in each image, but also provides a rich collection of biomarkers that can be used for the description of the deformations of arterial walls in image sequences. Three categories of biomarkers are extracted using the proposed models: geometrical features, energy features and motorial features.

Experiments on a newly developed aorta-related drug EDDF suggest that these biomarkers work well as diagnostic indicators and can be used effectively for the evaluation of drug effects. Most of the biomarkers have strong correlations with the structural deformations of aorta rings caused by the drug stimulation. By comparing the biomarker values calculated from the treatment group and the control group, it can be concluded that EDDF can effectively improve blood vessel reactivity of calcium overload rats to vasoactive agents. Different drugs can be compared quantitatively and objectively in the same way. To be objective, several kinds of possible artifacts of the algorithm that may cause some uncertainties in the results are thoroughly discussed and analyzed.

References

[1] Denk W, Strickler JH, Webb WW. Two-photon laser scanning fluorescence microscopy. Science 1990;248:73–6.

[2] Denk W, Piston DW, Webb WW. In: Pawley JB, editor. Handbook of biological confocal microscopy. New York: Plenum Press; 1995.

[3] Lin XS, Sun F, Ma H, Zhao JB, Jin L, Chen DY. Two-photon fluorescence imaging of rat aorta. Proceedings of SPIE 2000;4224: 7–12.

[4] Kwon HM, Sangiorgi G, Spangnoli LG. Experimental hypercholesterolemia induced ultrastructural changes in the internal elastic lamina of porcine coronary arteries. Atherosclerosis 1998;139:283–9.

[5] Masters B. Confocal microscopy and multi-photon excitation microscopy of human skin in vivo. Opt. Expr. 2001;8(1):2–11.

[6] Gilbert RJ, Hoffman M, Capitano A. Imaging of three-dimensional epithelial architecture and function in cultured CaCO2A monolayers with two-photon excitation microscopy. Microsc Res Tech 2000;51: 204–10.

[7] Arkas D, Becker D. Applications of spectral imaging: Detection and analysis of human melanoma and its precursors. Pigm Cell Res 2001; 14:2–8.

[8] Kass M, Witkin A, Terzopoulos D. Snakes: active contour models. Int J Comput Vis 1988;2(3):321–31.

[9] Hoch M, Litwinowicz P. A semi-automatic system for edge tracking with snakes. Vis Comput 1996;12:75–83.

[10] Menet S, Saint-Marc P, Medioni GB. Snakes: implementation and application to stereo. Image Understand Workshop 1990;720–6.

[11] Eviatar H, Somorjai R. A fast, simple active contour algorithm for biomedical images. Pattern Recognit Lett 1996;17:969–74.

[12] Klein A, Egglin TK, Pollak JS, Lee F, Amini A. Identifying vascular features with orientation specific filters and B-spline snakes. Comput Cardiol 1994;113–6.

[13] Chang CC, Hwang SM, Buehrer DJ. A shape recognition scheme based on relative distances of feature points from the centroid. Pattern Recognit 1991;24(11):1053–63.

[14] Wen YY, Zhang XC, Xu XR, Zhao GQ, Wan F. Action mechanisms of a new erythrocyte-derived depressing factor. Chin Sci Bull 2000; 45:2113–8.

[15] Serra J. Image analysis and mathematical morphology. New York: Academic Press; 1982.

[16] Rueckert D, Burger P, Forbat SM, Mohiaddin RD, Yang GZ. Automatic tracking of the aorta in cardiovascular MR images using deformable models. IEEE Trans Med Imaging 1997;16(5):581–90.

[17] Handa R, Ip HHS, Tang HY. Computerised analysis of aortic distensibility on computed tomography. Proceedings of the Conference on the Current Perspectives in Healthcare Computing; 1997. p. 157–65.

Jue Wang received the BE and MS degree from Department of Automation, Tsinghua University, Beijing, China in 2000 and 2002. Now he is a graduate student in Department of Electrical Engineering, University of Washington at Seattle. His research interests include image processing, computer vision, pattern recognition and multimedia network.

Liang Ji received the BA degree in physics from Tsinghua University (TU), Beijing, China and PhD degree in medical informatics from Aalborg University, Denmark. He worked in R&D Section of Beijing Nuclear Instrument Factory and in the Pattern Recognition and Automation Section of The MRC Human Genetics Unit, Edinburgh, Scotland, UK He has worked at TU since 1995 and is a professor of Institute of Information Processing, Department of Automation and Institute of Bioinformatics, TU. His research interests include bioinformatics, biomedical image analysis, pattern recognition and modernization of Traditional Chinese Medicine.

Xing-Sun lin received the BS and MS degree in Department of Physics, Tsinghua University, Beijing, China in 2000 and 2003. His research interests include radiological imaging, 3D imaging and microscopy.

Hui Ma, PhD, Professor, laser spectroscopist by training, current research interests are: optical microscopic techniques and their biomedical applications, fluorescence fluctuation spectroscopy.